Original Research

Journal of Advanced Veterinary Research
(2024) Volume 14, Issue 7, 1118-1125

Pumpkin seed and grape seed extracts ameliorate cyclophosphamide -induced spermatogenesis inhibition in rat model: Histomorphometrical, immunohistochemical, and ultrastructural approaches

Eman Mohamed Samy[1*], Muhamad Abd-Elraouf[2], Abdel-Baset I. El-Mashad[1], Shawky A. Moustafa[1], Ahmed A. Tantawy[1]

[1]*Department of Pathology, Faculty of Veterinary Medicine, Benha University, Toukh 13736, Egypt.*
[2]*Department of Pharmacognosy and Medicinal Plants, Faculty of Pharmacy, Al-Azhar University, Cairo 11884, Egypt.*

ARTICLE INFO

Recieved: 25 June 2024

Accepted: 30 July 2024

***Correspondence:**

Corresponding author: Eman Mohamed Samy
E-mail address: Eman.mohamed@fvtm.bu.edu.eg

Keywords:

Cyclophosphamide, PSE, GSE, Spermatogenesis arrest, Immunohistopathological, Ultrastructure.

ABSTRACT

This study investigated the protective efficacy of grape seed extract (GSE) and pumpkin seed extract (PSE) against cyclophosphamide (CP)-induced testicular toxicity in adult male albino rats, focusing on biochemical, histopathological, histomorphometrical, ultrastructural, and immunohistochemical perspectives. Thirty-six male albino rats were divided into six groups: Control, PSE, GSE, CP, CP + PSE, CP + GSE. Testicular tissues and serum samples were collected for analysis after 8 weeks. The CP group exhibited significant testicular damage with distorted seminiferous tubules (marked decline in diameters and germinal epithelial thicknesses), germ cell apoptosis, and disrupted spermatogenesis (decline in Johnsen's score and weak immunoexpression of PCNA in basal germ cells). Ultrastructurally, germ cells exhibited shrunken pyknotic nuclei and cytoplasmic aggregations of ribosomes with dilated or shrunken mitochondria. Spermatozoa displayed an irregular axoneme with loss of fibrous sheath. Furthermore, there were significantly decreased testosterone levels and increased oxidative stress markers (elevated malondialdehyde levels and decreased glutathione levels). In contrast, the CP + PSE and CP + GSE groups showed marked mitigation of these changes, resulting in a notable amelioration of oxidative stress markers, and testosterone levels, preservation of testicular architecture, and normalization of spermatogenic processes, along with elevated Johnsen score. Immunohistochemical analysis revealed an increase in PCNA in the CP + PSE and CP + GSE groups compared to the CP group. These findings suggested that GSE and PSE, owing to their antioxidant properties, could effectively reduce CP-induced testicular damage.

Introduction

The intersection of cancer treatment and reproductive health presents a complex challenge in modern medicine. Chemotherapy, while a cornerstone in the battle against cancer, often comes with adverse effects on fertility, particularly in males. Among the array of chemotherapeutic agents, CP stands out for its broad-spectrum efficacy but also its notorious side effect: the induction of testicular toxicity (Ghafouri-Fard *et al*., 2021). This toxicity was manifested in several forms, including oligospermia, azoospermia, and disruption of the spermatogenesis cycle, thereby posing a severe risk to male reproductive health (Oliveira *et al*., 2020).

The detrimental impact of CP on the testes is largely attributed to its metabolites. Phosphoramide mustard and acrolein contribute to its anticancer properties but are also implicated in its toxic side effects, mediated through the overproduction of reactive oxygen species (ROS), DNA damage, protein adduct formation, endoplasmic reticulum stress, and ultimately cellular dysfunction in testicular tissues (Zirak *et al*., 2019). In light of these concerns, there is a growing interest in identifying adjunctive treatments that can mitigate CP's reproductive toxicity without compromising its anticancer efficacy.

Pumpkin seeds from *Cucurbita pepo* have gained attention for their high nutritional and medicinal value. It is rich in unsaturated fatty acids, particularly omega fatty acids, and essential trace elements like magnesium, iron, and zinc (Srivastava *et al*., 2021). PSE exhibits antioxidant, anti-inflammatory, and immunomodulatory properties (Vinayashree and Vasu, 2021). These characteristics have positioned PSE as a potential therapeutic agent for protecting spermatogenic function, especially in the context of chemotherapy-induced damage (Elfiky *et al*., 2012; Shaban and Sahu, 2017).

Similarly, grape seed derived from *Vitis vinifera*, is a rich source of polyphenols and flavonoids (Gupta *et al*., 2020). These compounds are known for their potent antioxidant capabilities, which include scavenging free radicals, reducing lipid peroxidation, and modulating inflammatory responses (Tabeshpour *et al*., 2018). GSE has shown promising results in enhancing mitochondrial enzyme activities and improving testicular histopathology, suggesting its potential as a gonadoprotective agent against various testicular injuries induced by cadmium chloride and bisphenol A (Morsi *et al*., 2020; Malek *et al*., 2022).

This study aimed to investigate the roles of GSE and PSE in combating CP-induced testicular toxicity in adult male albino rats via biochemical, histopathological, histomorphometrical, ultrastructural, and immunohistochemical analyses.

Materials and methods

Animals

The study was conducted on 36 apparently healthy adult male albino rats weighing 300 ±10g, obtained from the Animal House, Faculty of Veterinary Medicine, Zagazig University, Egypt. Rats were acclimated for one week before the experiment at a temperature approximately 25±5°C, humidity 60±5% with a 12 h light/dark cycle and provided with standard feed and water ad libitum. All experimental procedures were carried out in accordance with the international guidelines for laboratory animal care and were approved by the Research Ethical Committee of the Faculty of Veterinary Medicine, Benha University (Ethical Approval Number: BUFVTM 06-03-23).

Chemicals

Cyclophosphamide (Endoxan) was produced by Baxter Oncology GmbH Kantstrasse2 D-33790 Halle, Germany, as vial 1g contains 1.069 g cyclophosphamide monohydrate equivalent to 1g anhydrous cyclophosphamide. The drug was dissolved in saline before intraperitoneal administration.

ISSN: 2090-6277/2090-6269/

Grape seed extract (GSE) and pumpkin seed extract (PSE) preparation

The grape and pumpkin fruits were procured from a local market and authenticated by the Department of Horticulture, Faculty of Agriculture, Benha University, Egypt. Seeds were manually removed, dried, and powdered. Then ethanolic grape seed extract was prepared (Badavi *et al*., 2013) and the ethanolic pumpkin seed extract was produced (Xanthopoulou *et al*., 2009).

Experimental design

Rats were randomly divided into six equal groups (N=6):
Group I (Control), rats were injected intraperitoneally with 0.5 ml of 0.9% saline solution weekly from the second week till the end of the experiment.
Group II (PSE), rats were administrated PSE orally at a dose of 300 mg/kg b.wt daily for 8 weeks (Aghaei *et al*., 2014).
Group III (GSE), rats were administrated GSE orally at a dose of 150 mg/kg b.wt daily for 8 weeks (Aboul-Ela and Omara, 2014).
Group IV (CP), rats were injected intraperitoneally with CP (60 mg/kg b.wt) weekly from the second week till the end of the experiment (Torabi *et al*., 2017).
Group V (PSE + CP), rats were administered PSE orally at a dose of 300 mg/kg b.wt daily and injected intraperitoneally with CP (60 mg/kg b.wt) weekly from the second week till the end of the experiment.
Group VI (GSE + CP), rats were administered GSE orally 150 mg/kg b.wt/ daily and injected intraperitoneally with CP (60 mg/kg b.wt) weekly from the second week till the end of the experiment.

Body and testis weights

The body and testicular weights were recorded in this study. The body weights of each animal were recorded at the start and end of the experiment. At the end of the experiment, the testes were dissected and weighed. The Relative Testicular Weight (RTW) % was calculated.
Relative Testicular Weight = organ weight/ body weight x 100

Hormonal analysis

At the end of the experiment, blood samples were collected from the retro-orbital venous plexus of each rat into gel and clot activator tubes. Serum was obtained by blood centrifugation at 3000 rpm for 15 min. The serum testosterone level was measured by enzyme-linked immunosorbent assay (ELISA) methods (Teilmann *et al*., 2014), using commercial kits from Randox (UK). Testosterone value is expressed as nmol/L.

Estimation of oxidative stress markers

The testicular homogenate was obtained by grinding a small piece (1g) of freshly excised tissue in 10 volumes of ice-cold PBS saline solution, using a tissue homogenizer. After that, it was centrifuged at 4,000 rpm for 15 minutes at 4°C. Once done, the supernatant was removed and stored at -80°C until needed for the determination of malondialdehyde (MDA) levels and reduced glutathione (GSH) levels (Taghizadeh *et al*., 2020) by a SPECTROstar Nano spectrometer (BMG LAB-TECH, USA) , using commercial Biodiagnostic kits (Biodiagostic, Giza, Egypt).

Histopathological examination and testicular damage scoring

To evaluate the histological alteration of the seminiferous tubules, the testes of rats in all groups were collected and immediately fixed overnight in Bouin's solution, then routinely processed to prepare 5 µm thick paraffin sections and stained with hematoxylin and eosin stain (Bancroft and Layton, 2019). The severity of lesions was scored as follows: (−) absence of the lesion = 0%, (+) mild > 0–25%, (++) moderate > 25–50%, and (+++) severe > 50–100% of the examined tissue sections (Tohamy *et al*., 2021).

Spermatogenesis assessment through Johnsen Score

According to Johnsen (1970), 100 seminiferous tubules were examined in each rat to evaluate spermatogenesis using the Johnsen scoring system (Table 1). To calculate the mean Johnsen's score in each rat testis, the sum of all the recorded scores was divided by the total number of the examined seminiferous tubular (100).

Table 1. Johnsen scoring system for spermatogenesis assessment.

Score	Level of spermatogenesis (seminiferous tubule feature)
10	Complete spermatogenesis with many spermatozoa present
9	Slightly impaired spermatogenesis, many late spermatids, disorganized epithelium
8	Few spermatozoa per tubule, few late spermatids
7	No spermatozoa, no late spermatids, many early spermatids
6	No spermatozoa, no late spermatids, few early spermatids
5	No spermatozoa or spermatids, many spermatocytes
4	No spermatozoa or spermatids, few spermatocytes
3	Spermatogonia only
2	Presence of Sertoli cells only
1	No seminiferous epithelium.

Morphometric analysis

Morphometric analysis of the seminiferous tubules was conducted by measuring the diameter and epithelial thickness in a total of 100 tubules for each group (10 tubules in each testicular section and 10 sections per group) (Karimi *et al*., 2018), using the ImageJ program (ImageJ Version 1.45 s, NIH, USA). The mean diameter of the seminiferous tubule (ST) was calculated through calculating the averages of the lengths of the short edge and the long edge (two diameters perpendicular to each other) measured in µm.
Average ST diameter (µm) = ST diameter $(\mu m)_1$ + ST diameter $(\mu m)_2/2$

The germinal epithelial thickness (ET) of the seminiferous tubules was conducted by measuring the thicknesses of the epitheliums from the four sides and the four angles in µm, and the averages of the thickness lengths were calculated.
Average ET (µm) = ET length $(\mu m)_1$ + ET length $(\mu m)_2$+ ET length $(\mu m)_3$+ ET length $(\mu m)_4/4$

Immunohistochemical analysis

Immunohistochemistry for proliferating cells nuclear antigen (PCNA) was performed with monoclonal anti-PCNA antibody (clone PC10; Dako, Denmark, Glostrup, Denmark, diluted in the ratio of 1:200) as described earlier by D'Andrea *et al*. (2008).

Ultrastructural analysis

Small pieces of the testicular tissue were directly fixed in fresh 2.5% glutaraldehyde buffered with 0.1M phosphate buffer at pH 7.4 for 2 hours at 4ºC. Then postfixed in 1% osmium tetroxide in the same buffer for one hour at 4ºC. After that, the tissue was dehydrated in an ethanol series, embedded in Epon 812 resin (Woods and Stirling, 2019). Semithin sections (1 um thick) were stained with 1% toluidine blue and examined by a light microscope to ensure proper orientation. Ultrathin sections were contrasted with uranyl acetate and lead citrate to be examined with TEM (Jeol 1400 plus, Tokyo, Japan) in the Electronic Microscope Lab, Faculty of

Agriculture, Mansoura University.

Statistical analysis

All data analyses were performed using SPSS for Windows Version 22.0 (IBM Corp. Released 2013). One-way analysis of variance (ANOVA) was used for comparison between groups followed by the least significant difference (LSD) post hoc test. The data were expressed as mean ± standard error (SE) and P ≤ 0.05 was considered statistically significant.

Results

Impact of PSE and GSE on body and testicular weights

There was a notable significant reduction in the body and testicular weights at the end of the experiment in the CP-treated group compared to the control group. This reduction was significantly mitigated in the CP + PSE and CP + GSE groups (Table 2).

Table 2. Comparative analysis of each experimental group's average body and testicular weights.

Groups	Body weight (g)		Testes weight	
	Initial	Final	Absolute (g)	Relative (%)
Control	301.3±4.177 ^{a}	370.00±4.80^{b}	1.81±0.09^{a}	0.55±0.03^{a}
PSE	304.2±5.224 ^{a}	428.70±2.19^{a}	1.93±0.04^{a}	0.53±0.00^{a}
GSE	296.5±3.594 ^{a}	368.70±2.91^{b}	1.83±0.16^{a}	0.55±0.01^{a}
CP	302.0±5.916 ^{a}	201.30±5.70^{d}	0.96±0.06^{c}	0.41±0.00^{b}
CP+PSE	299.8±4.607 ^{a}	289.70±3.18^{c}	1.51±0.02^{b}	0.49±0.00^{a}
CP+GSE	299.8±4.615 ^{a}	275.30±10.09^{c}	1.49±0.04^{b}	0.49±0.05^{a}

Values (mean ± S.E) within the same column that has the same superscript letter indicate no significant difference (P>0.05).

Hormonal analysis

Compared to control group, there was a significant decrease in the testosterone level of the CP-treated group when compared to the control group (P <0.001), and other treated groups being significantly higher compared to the CP group (P <0.05) as shown in Fig. 1.

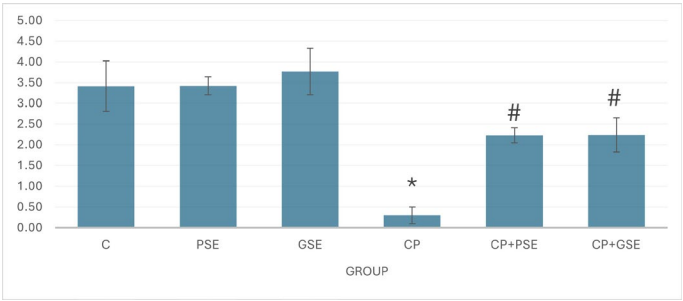

Fig. 1. Effect of PSE and GSE on CP-induced reduction in serum testosterone level. Values are expressed as mean ± S.E. * P< 0.001 compared with control; # P< 0.05 compared with CP.

Effect of PSE and GSE on CP-induced testicular oxidative stress

CP treatment caused a significant increase in MDA levels (P <0.0001) in testicles with consequent reductions in GSH levels (P <0.001) compared to control. Pretreatment with PSE and GSE caused a significant reduction in MDA levels (P <0.001) with a marked increase in GSH levels (P <0.05). This data is presented in Table 3.

Table 3. Effect of cyclophosphamide, PSE and GSE on testicular MDA and GSH levels.

Group	MDA level (nmol/g)	GSH level (nmol/g)
Control	9.12±2.27^{c}	250.80±20.34^{a}
PSE	8.47±0.56^{c}	294.00±19.58^{a}
GSE	8.43±0.62^{c}	279.90±46.3^{a}
CP	40.73±1.15^{a}	38.75±1.94^{c}
CP+PSE	27.82±1.336^{b}	151.00±8.97^{b}
CP+GSE	27.66±1.78^{b}	148.70±3.46^{b}

Values are expressed as mean ± SE. Differences within the same column that have different superscript letters are considered statistically significant (P<0.05).

Histopathological findings and testicular damage scoring

The majority of the examined testicular sections in the control group showed a normal histological structure of seminiferous tubules. These tubules were lined by stratified germinal epithelium with abundant spermatozoa into the lumens (Fig. 2A). Similarly, almost all examined testicular sections of the PSE and GSE groups also displayed well-defined seminiferous tubules at different stages of spermatogonial cells (Fig. 2B, C).

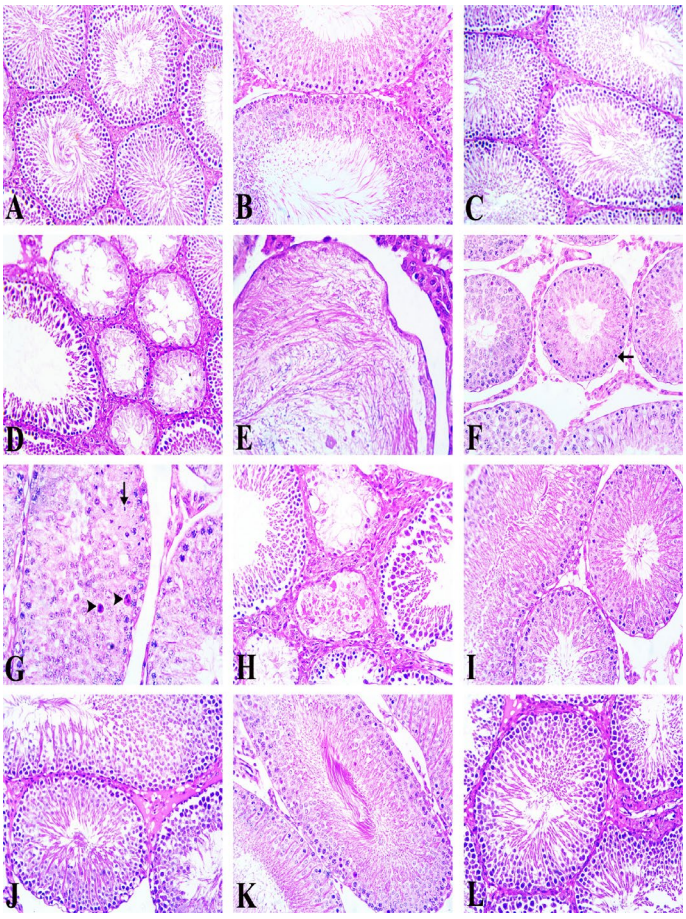

Fig. 2. Representative photomicrograph of H&E-stained testicular sections of different experimental groups, x 200. (A) Control group showing normal seminiferous tubules were lined by stratified germinal epithelium with abundant luminal spermatozoa. (B, C) PSE and GSE groups respectively, exhibiting well-defined seminiferous tubules at different stages of spermatogonial cells. (D- H) CP group, (D) showing atrophied seminiferous tubules lined by one or two layers of vacuolated germinal epithelium, with no spermatogenesis. Note the diffuse interstitial tissue proliferation, (E) sperm stasis in the lumen of the atrophied seminiferous tubules, (F) spermatogonia cells had darkly stained nuclei with cytoplasmic vacuolations (arrow), Notice irregular and undulant basement membranes with spaces between them and basal germ cells, with the absence of primary and secondary spermatocytes in some tubules, (G) within the lumen of some seminiferous tubules exfoliated germ cells and apoptotic germ cells (arrowhead). Note the arrested spermatocyte at various stages of development with wide intercellular spaces (arrow). The interstitial Leydig cells show cytoplasmic vacuolation, (H) necrosed seminiferous tubules filled with fibrillar eosinophilic debris. (I, J) PSE + CP group revealing (I) normal histoarchitecture of seminiferous tubules with mild cytoplasmic vacuolation, (J) and mild interstitial edema. (K, L) GSE + CP group showing (K) remarkable preservation of the germinal epithelium with different stages of spermatogenesis, few apoptotic cells in between well-organized intact germ cells, few intercellular spaces, (L) and mild interstitial edema.

Meanwhile, most of the examined testicular sections of the CP group

revealed marked testicular damage in the form of testicular atrophy and even necrosis. The atrophied seminiferous tubules were reduced in size with a significant loss of germ cells. They were lined by one or two layers of the vacuolated germinal epithelium with no spermatogenesis process and luminal sperms. Diffuse interstitial tissue proliferation was prominent in between these atrophied tubules (Fig. 2D). Sperm stasis was infrequently seen in the lumen of these atrophied tubules (Fig. 2E). Moreover, some seminiferous tubules showed spermatogenesis arrest with the absence of some differential stages as primary and secondary spermatocyte and luminal spermatozoa. Some of these seminiferous tubules had irregular, undulant basement membranes with spaces between these basement membranes and the basal spermatogonia. Most of these spermatogonia had pyknotic nuclei with cytoplasmic vacuolation (Fig. 2F). Most seminiferous tubules were packed with exfoliated germinal epithelium and showed shrunken apoptotic germ cells with hyper-eosinophilic cytoplasm and fragmented nuclei. Furthermore, these seminiferous tubules showed arrest of spermatocytes at various stages of development with wide intercellular spaces (Fig. 2G). Furthermore, there were focal necrosis of seminiferous tubules was accidentally seen. These necrotic seminiferous tubules revealed a significant reduction in spermatogenesis and were lined only with very few spermatogonia or only Sertoli cells. Most of these tubules had thickened basement membranes and their lumina were filled with fibrillar eosinophilic necrotic debris (Fig. 2H). The interstitial Leydig cells had cytoplasmic vacuolation. In addition to the seminiferous tubule damage induced by CP, severe vascular changes were also seen in the examined testicular sections of rats treated with CP. These vascular changes were congestion of intertubular blood vessels with injured endothelial cells, thrombosis, and interstitial edema.

Almost all the examined PSE + CP group testicular sections revealed normal histoarchitecture of the seminiferous tubules with abundant luminal spermatozoa. However, mild degenerative changes were detected in some seminiferous tubular epithelium represented by cytoplasmic vacuolation (Fig. 2I), mild congestion, and minimal interstitial edema were infrequently seen (Fig. 2J). The majority of testicular sections from the GSE + CP group showed well-preserved germinal epithelium with various stages of spermatogenesis. However, some sections revealed a few apoptotic germ cells with fragmented nuclei and highly eosinophilic cytoplasm, along with cytoplasmic vacuolations in some germ cells (Fig. 2K). Additionally, mild interstitial edema was occasionally observed (Fig. 2L).

The histopathological alterations in H&E-stained testicular sections of different experimental groups were represented as a score (Table 4). The CP-treated group had the highest score for the recorded lesions in the seminiferous tubules particularly tubular atrophy, necrosis, germ cell apoptosis, tubular vacuolation, germ cell loss and giant cell formation in addition to vascular damage. In contrast, pretreatment with PSE or GSE groups was related to a reduction in these scores, indicating the gonadoprotective effect of these extracts against CP-induced testicular injury.

Spermatogenesis assessment through the Johnsen scoring

A notable significant ($p < 0.0001$) decrease in Johnsen's testicular score was evident in the CP group, indicating impaired spermatogenesis. This impairment is further reflected in the higher prevalence (58.4%, and 33.2%) of lower Johnsen scores (3-4 and 5-6) when compared to the control group which exhibited the highest proportion of higher Johnsen scores (9-10). However, these high scores were not recorded in the CP group. Conversely, pretreatment with PSE or GSE exhibited improved Johnsen scores compared to the CP group alone which was evidenced by the return of scores 9-10 in 39.2% and 49.9% of the tubules, respectively. This is visually captured in Fig. 3A, where the mean Johnsen score for each group is represented by bars, and in Fig. 3B, which shows the frequency distribution of the scores, across the groups.

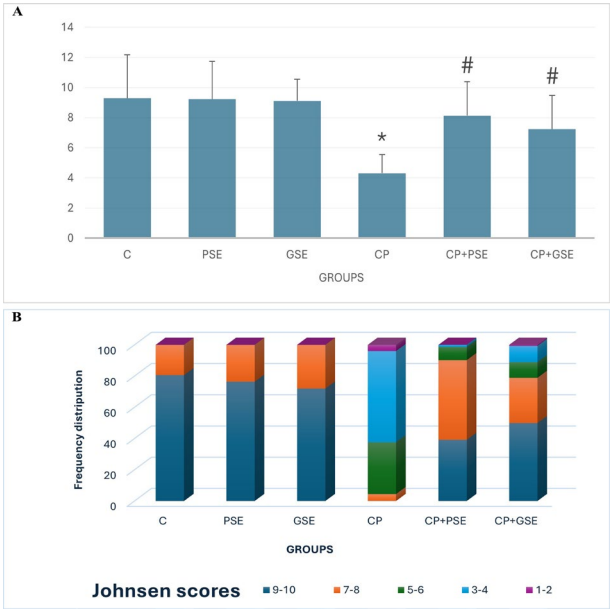

Fig. 3. (A) Effect of cyclophosphamide, PSE and GSE on spermatogenesis in each experimental group through evaluation of Johnsen score. Data was analyzed by one-way ANOVA followed by post hoc test and $p < 0.05$ was significant. * $P < 0.001$ compared with control; # $P < 0.001$ compared with CP. (B) Frequency distribution of Johnsen's testicular scores in rats' experimental groups.

Morphometric analysis

Effect of CP, PSE, and GSE on seminiferous tubule diameter and epithelium thickness

The result of the histomorphometric analysis of seminiferous tubule diameter and epithelium thickness were illustrated in Table 5. In terms of seminiferous tubular diameter, CP treatment caused a notable reduction compared to the control group. However, when rats were pretreated with

Table 4. Comparative scoring of the testicular histopathological changes in each treatment group.

Lesion	Control, PSE, GSE	CP	CP+PSE	CP+GSE
Tubular atrophy	-	+++	+	+
Tubular necrosis	-	++	+	+
Germ cell apoptosis	-	+++	+	+
Tubular vacuolation	-	+++	+	+
Germinal cells desquamation & giant cell formation	-	+++	+	+
Sperm stasis	-	+	-	-
Interstitial edema	-	++	+	+
Interstitial fibrosis	-	+	-	-
Diffuse Interstitial proliferation	-	+	-	-
Vascular lesion & thrombus formation	-	+++	+	+

(-): Normal histology, (+): Mild, (++): Moderate, (+++): Severe.

PSE or GSE, statistically significant increases in the tubular diameters were recorded compared to CP-treated rats. Furthermore, the germinal epithelial thickness of seminiferous tubules in the PSE and GSE pretreatment groups were nearly similar to those of the control rats. Conversely, in rats treated with CP, a significant reduction in the germinal epithelium thickness was observed compared to the control. Interestingly, pretreatment with PSE or GSE significantly mitigated the reduction in the germinal epithelium thickness when compared to CP-treated group.

Table 5. Comparative analysis of each experimental group's average seminiferous tubule diameter and germinal epithelium thickness.

Group	STD (µm)	GET (µm)
Control	324.75±5.02^{a}	97.35±2.79^{b}
PSE	308.90±5.95^{b}	96.19±2.55^{b}
GSE	316.96±6.24^{ab}	106.12±3.65^{a}
CP	225.46±3.17^{e}	71.79±1.37^{d}
CP+PSE	270.06±4.90^{c}	87.96±2.22^{c}
CP+GSE	250.31±4.98^{d}	82.01±2.3^{c}

Values are expressed as mean ± SE. Differences within the same column that have different superscript letters are considered statistically significant (P<0.05). STD: seminiferous tubule diameter and GET: germinal epithelium thickness.

Immunohistochemical evaluation

The seminiferous tubules of the control group exhibited marked expression of PCNA characterized by intense brown labelling of spermatogonia and spermatocyte nuclei (Fig. 4A). Similar expression was observed in PSE and GSE groups. Meanwhile, CP-treated rats showed weak PCNA-positive reactions for spermatogonia and spermatocyte nuclei in seminiferous tubules (Fig. 4B). Interestingly, rats co-treated with PSE (Fig. 4C) or GSE (Fig. 4D) revealed strong positive brown expression of PCNA in nuclei of the basal spermatogenic cells compared to CP group.

Ultrastructural Observations

Transmission electron microscopy of the testes of the control group showed spermatogonia with large oval nuclei resting on a regular basement membrane. The primary spermatocyte had normal large euchromatic nuclei with synaptonemal complex and a thin rim of cytoplasm containing an aggregation of abundant small mitochondria. The early spermatid had an intact plasma membrane, rounded euchromatic nuclei covered by the acrosomal cap and many peripherally situated mitochondria. The cross-section of spermatozoa displayed an intact axoneme formed from nine doublets of microtubules and two central singlets. The axoneme was enclosed by a dense fibrous cap and intact plasma membrane sheath (Fig. 5A-D).

The seminiferous tubules of CP displayed significant ultrastructural changes affecting germ cells that separated from the thickened irregular basement membrane leaving large spaces. Most germ cells were lost due to complete cytolysis with the presence of necrotic debris of ruptured fragmented cells and apoptotic bodies (membrane-bounded cytoplasmic ribosome and vacuoles). The primary spermatocyte revealed an irregular membrane bounding with loss of cellular tight junction and increased intercellular space. Additionally, there were abundant cytoplasmic and nuclear changes, including an irregular shrunken, pyknotic nucleus with clumping of the synaptonemal complex, and cytoplasmic aggregations of ribosome with dilated or shrunken electron-dense mitochondria. Most spermatozoa exhibited deformity with complete lysis and loss of its normal ultrastructure. Others showed irregularity with shrunken irregular axoneme, loss of fibrous caps and dilated plasma membranes, or ruptured head acrosomal caps and dilated tails (Fig. 6A-F).

In the CP + PSE group, most spermatogonia appeared normal with an intact nucleus and normal mitochondria with minimal cytoplasmic vacuolation. However, some of them showed separation from the basement membrane, leaving intercellular spaces. Many spermatocytes had intact centrally located nuclei with minimal mitochondrial dilation, while others had irregularly shaped nuclei. Additionally, some spermatocytes exhibited lysis with extracellular diffusion of mitochondria and ribosomes. Spermatozoa varied in size with normal axoneme and only minimal irregularity in fibrous and plasma membrane sheaths was observed (Fig. 7A-D).

In the CP+GSE group, most spermatogonia had an intact nucleus and numerous mitochondria. However, some of them showed irregularities with the presence of a few cytoplasmic vacuoles, variable-sized

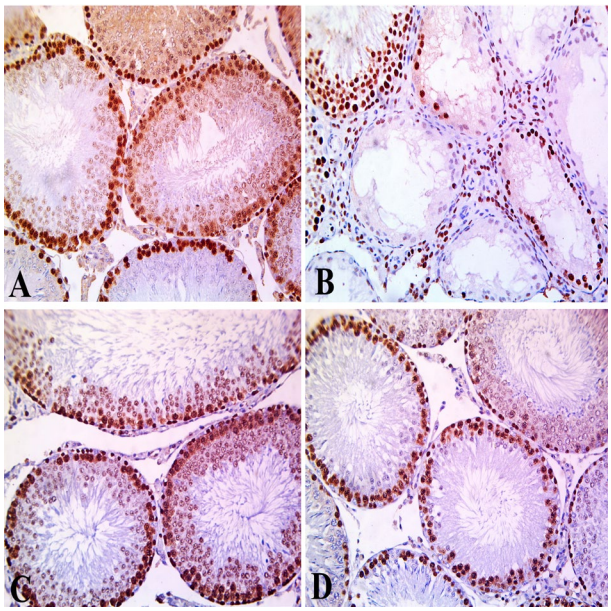

Fig. 4. Representative photomicrograph of immunohistochemical staining of PCNA in testicular sections of different experimental groups, x 200. (A) Control group, marked expression of PCNA was characterized by intense brown labelling of spermatogonia and spermatocytes in seminiferous tubules. (B) CP treated group, mild positive reaction for PCNA expression in seminiferous tubules. (C) CP+PSE treated group, strong positive brown expression of PCNA in nuclei of the basal spermatogenic cells. (D) CP+GSE treated group, strong positive immunoreactivity in nuclei of the basal spermatogenic cells.

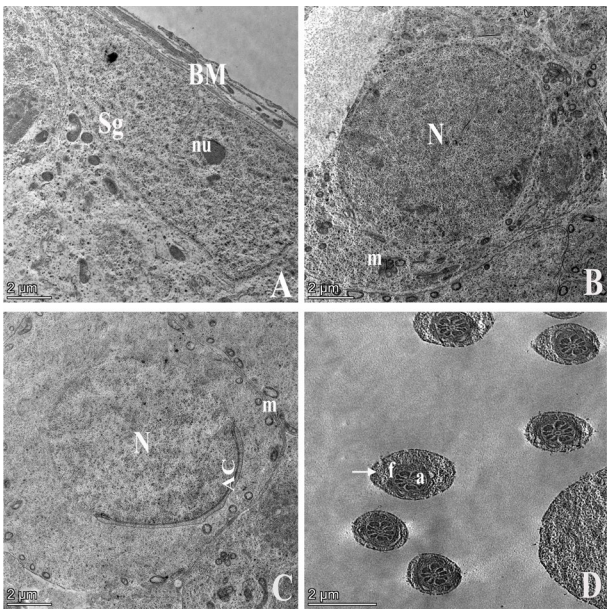

Fig. 5. Representative TEM micrographs of control testis showing (A) large spermatogonia (Sg) with oval nucleolus (nu) resting on a regular basement membrane (BM). (B) spermatocyte showing normal large euchromatic nuclei (N) with synaptonemal complex and a thin rim of cytoplasm containing an aggregation of abundant small mitochondria (m). (C) spermatid showing intact plasma membrane, intact rounded nucleus (N) with acrosomal cap (AC) and many peripherally arranged mitochondria (m). (D) cross section of spermatozoa showing intact axoneme (a) enclosed within dense fibrous cap (f) and intact plasma membrane sheath (arrow).

mitochondria, and electron-dense lysosomes. Spermatocytes with a divided nucleus, minimal cytoplasmic vacuolation, a massive number of ribosomes, and peripherally arranged mitochondria with mild dilation were also detected. Normal spermatozoa with only partial irregularity in the fibrous sheath were observed (Fig. 8A-D).

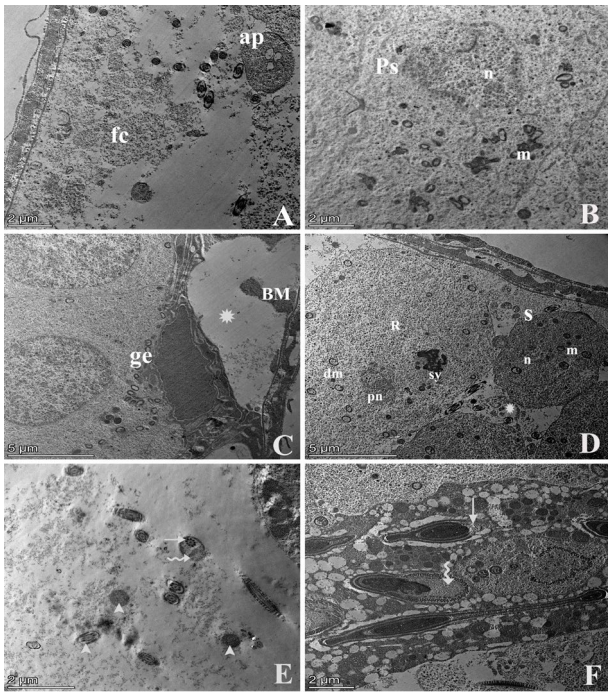

Fig. 6. Representative TEM micrographs of testis from CP group. (A) seminiferous tubules showing complete lysis and disruption of germ cell lining, loss of most cells and necrotic debris of rupture and fragmented cells (fc) with the presence of the apoptotic body (ap). (B) primary spermatocyte (Ps) with irregular membrane bounding, irregular small-sized nucleus (n) and aggregation of dilated or shrunken, electron-dense mitochondria (m). (C) separation of germ cells (ge) from the thickened basement membrane (BM) leaving a large space (star). (D) loss of normal ultrastructural germ cell lining with dilated basement membrane, dilated primary spermatocytes with shrunken, pyknotic nucleus (pn), increased ribosome amount (R), dilation of scattered mitochondria (dm), clumping of synaptonemal complex (sy), adjacent to this cells, shrunken cells (S) with shrunken nucleus (n) and few mitochondria (m) in addition to loss of cellular tight junction with increase intercellular space (star). (E) spermatozoa exhibited deformity with either shrunken irregularly shaped axoneme (thin arrow) with loss of fibrous cap and dilated plasma membrane (zigzag arrow), other spermatozoa showed complete lysis and loss of its normal ultrastructure (arrowhead). (F) deformation of the mature spermatozoa with either rupture of the head acrosomal cap (thin arrow) or dilation of the tail (zigzag arrow).

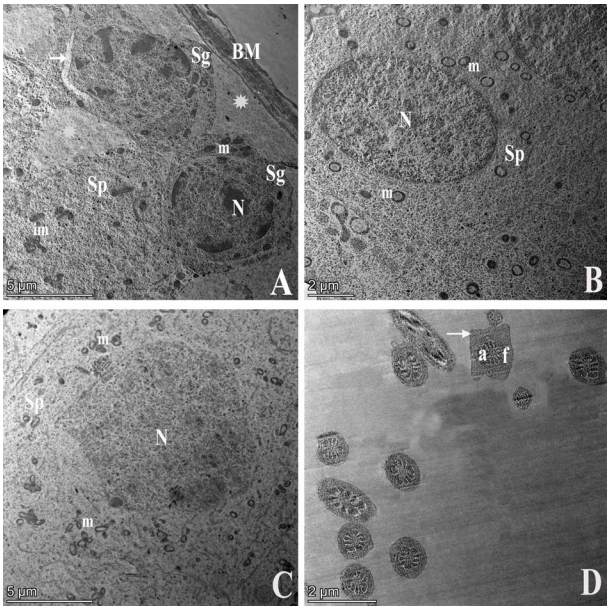

Fig. 7. Representative TEM micrographs of CP + PSE group. (A) seminiferous tubule showing separation of spermatogonia (Sg) from the basement membrane (BM) leaving wide intercellular space (star), spermatogonia mostly appeared normal with intact nucleus (N), mitochondria (m) and presence of minimal cytoplasmic vacuolation (arrow) while spermatocytes (Sp) showing either complete loss of nucleus with irregular shaped mitochondria (im) or cell lysis with presence of wide intercellular space (star). (B) spermatocyte (Sp) showing intact centrally located nucleus (N) with minimal mitochondrial dilation (m). (C) spermatocytes (Sp) with irregularly shaped nucleus (N) and aggregation of mitochondria (m). (D) spermatozoa showing variable-size with normal axoneme (a) and few irregular fibrous (f) and plasma membrane sheath (arrow).

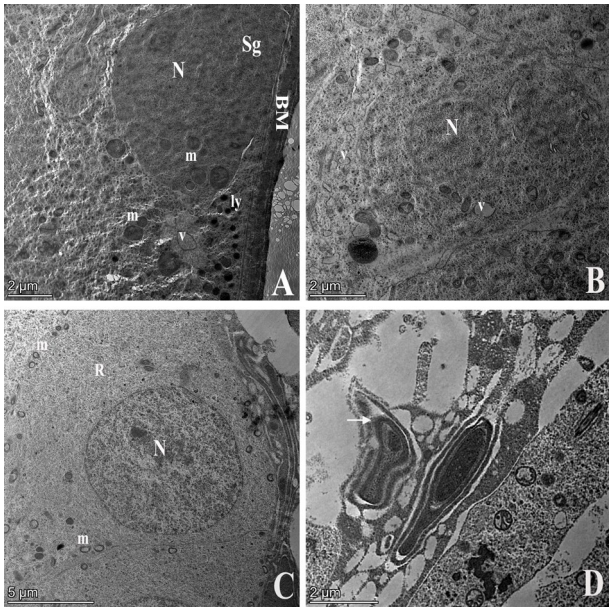

Fig. 8. Representative TEM micrographs of testes from CP + GSE group. (A) seminiferous tubule showing large spermatogonia (Sg) rested in regular basement membrane (BM) with intact nucleus (n) and numerous mitochondria (m), increased electron-dense lysosomes (ly), variable-sized mitochondria (m) and presence of a few cytoplasmic vacuoles (v). (B) enlarged germ cell with divided nucleus (N) minimal cytoplasmic vacuolation (v). (C) spermatocyte with intact nucleus (N), a massive amount of ribosome (R), and peripherally arranged mitochondria (m) with mild dilation. (D) spermatozoa with partial irregular fibrous sheath (arrow).

Discussion

This study highlights the significant adverse effects of cyclophosphamide (CP) and the possible protective roles of PSE and GSE on male reproductive health. CP-induced reproductive toxicity with impaired spermatogenesis, the main cause of male infertility, despite its effectiveness in treating neoplastic and immunosuppressive diseases (Zhao *et al*., 2015). Therefore, potential protective agents are needed to reduce testicular injury caused by CP and test their efficacy in preserving fertility for cancer survivors aiming to resume their normal reproductive life after chemotherapy (Ghobadi *et al*., 2017).

As recorded in this study, weight loss is a common side-effect of cyclophosphamide therapy. Mechanisms responsible for this include the direct effect of CP on energy metabolism and its antiproliferative effects on adipocyte progenitors (Myers *et al*., 2017). Testicular weight is a critical indicator of normal spermatogenesis and reproductive health which is often measured in reproductive studies (Hassanzadeh-Taheri *et al*., 2019). In the present study, CP administration was associated with significantly decreased testicular weight compared with the control group, these results were inconsistent with Torabi *et al*. (2017). Furthermore, CP induced drastic microscopical changes in the testicular tissue where seminiferous tubular atrophy, spermatogenesis arrest, germ cell apoptosis, and multinucleated giant cell formation were frequently observed. This testicular damage was reflected in the result of the histomorphometric analysis where there was a significant decline in the seminiferous tubule diameters, tubular epithelial thickness, and Johnsen score, which was matched with previous studies (Kamarzaman *et al*., 2013; Salimnejad *et al*., 2018). Additionally, the ultrastructural examination of the seminiferous tubules revealed abundant cytoplasmic and nuclear changes, including a shrunken pyknotic nucleus, and cytoplasmic aggregations of the ribosome with dilated or shrunken electron-dense mitochondria. These results were inconsistent with Moustafa *et al*. (2020).

The recorded testicular damage induced by CP may be elucidated by generating free radicals and suppressing antioxidants which are evident by a significant decrease in GSH level with marked elevation in MDA level.

These findings were also recorded by Cengiz *et al*. (2020). The toxic effect of CP is also attributed to phosphoramide mustard, which interacts with the N7 of guanine on opposing strands of DNA. Thus, the cross-linking of DNA occurs, resulting in preventing both DNA replication, gene transcription, hindrance of cell proliferation, and induction of cell apoptosis (Dabbish *et al*., 2024). In the present study, the immunohistochemical analysis of PCNA revealed a weak positive reaction of the basal germ cell nuclei in the majority of examined testicular sections, reflecting the damaging effect of CP on the DNA of the germ cells. These results were parallel with Adana *et al*. (2022) where PCNA (Proliferating Cell Nuclear Antigen) is a nuclear matrix protein involved in DNA synthesis and repair during spermatogenesis and used as a marker for diagnosing germinal arrest due to DNA synthesis deterioration (Pan and Zhang, 2021). The present study recorded a significant reduction in testosterone hormone levels. The low testosterone level was commonly associated with impaired spermatogenesis and germ cell apoptosis as the normal testosterone level acts as a cell survival factor, in some way protecting germ cells from apoptotic death. A similar result was reported by Potnuri *et al*. (2018). Moreover, the ultrastructural findings revealed CP-induced marked sperm deformities such as irregular axoneme, loss of fibrous cap, dilated plasma membrane, ruptured head acrosomal cap and dilated tail. This could be attributed to the sensitivity of spermatozoa to lipid peroxidation and oxidative stress induced by CP due to their high concentrations of polyunsaturated fatty acids and low levels of antioxidants, which affected sperm integrity and increased sperm abnormalities (Lu *et al*., 2015; Ghobadi *et al*., 2017).

To prevent the detrimental effects of CP on the testes, it is highly recommended to use it combined with other natural byproducts with strong gonadoprotective activity (Singh *et al*., 2014). In this study, PSE pretreatment greatly negated the harmful effect of CP on the testicular tissue. There were improvements in the testicular architecture where almost all seminiferous tubules exhibited active spermatogenesis and abundant luminal spermatozoa. These results were in line with Ofoego *et al*. (2019). This mitigating effect was reflected in testicular weight which significantly increased compared with the CP-treated group. This finding was also recorded by Hashemi (2013). Similarly, there was a significant alleviation in the histomorphometric parameters such as seminiferous tubule diameters, tubular epithelial thickness, and Johnsen score which significantly increased compared with the CP-treated group. The electron microscopical findings confirmed the protective effect of the PSE where most germ cells had intact nuclei and normal mitochondria. The protective effect of the PSE could be attributed to the antioxidant and free radical scavenging activities as it is rich in Phenolic compounds, vitamins E and A, and Carotenoids that break down the oxidative chain reaction and increase the body's capacity to fight free radical-induced oxidative stress (Mohammadi *et al*., 2013). This opinion was supported by the testicular oxidative stress assessment status where the GSH level was significantly increased while the MDA level was markedly decreased. Similar results were in parallel with Hamdi (2020). Furthermore, PSE enhanced germ cell proliferation and protected against DNA damage, evidenced by marked increases in PCNA immunoexpression in the basal germ cell nuclei compared with the CP-treated group. These results were consistent with Mousa *et al*. (2023). In addition, PSE promoted spermatogenesis progression through improved testosterone levels compared to the CP-treated group. These findings were in line with Ofoego *et al*. (2019). This effect could be attributed to the high concentrations of squalene in the Pumpkin seeds, which is a precursor of steroid hormones such as testosterone. Additionally, pumpkin seeds are rich in triterpene, a precursor of vitamin D that has been shown to increase testosterone levels in both humans and experimental animals (Nimptsch *et al*., 2012). Moreover, PSE reduced the ultrastructural sperm deformities induced by CP, where most spermatozoa had normal axonema with minimal irregularities in the fibrous and plasma membranes. This effect could be attributed to PSE containing an abundant amount of oleic acid, a monounsaturated fatty acid that reduces the susceptibility of the spermatozoa to lipid peroxidation (Adsul and Madkaikar, 2021).

Similarly in the current study, pretreatment with grape seed extract substantially alleviated the CP-induced histological alterations in the testicular tissue, where most seminiferous tubules displayed normal spermatogenesis with different stages of germ cells. These results were consistent with Morsi *et al*. (2020). The ameliorative effect of the GSE on the testicular histoarchitecture was reflected in the testicular weight which significantly increased. Moreover, the result of the histomorphometric analysis revealed improvement in the recorded histomorphometric parameters where seminiferous tubule diameter, germinal epithelium thickness and mean Johnsen score were significantly increased, indicating active spermatogenesis. These results were in line with Sönmez and Tascioglu (2015). The testosterone level was associated with normal differentiation of the germ cells. In the current study, GSE pretreatment significantly increased the testosterone levels compared to the CP-treated group. The electron microscopical findings confirmed the active spermatogenesis in the GSE pretreated group, where most spermatocytes had divided nuclei and numerous ribosomes. In addition, GSE pretreatment ameliorated the deteriorating effects of CP on sperm morphology where most spermatozoa had normal ultrastructural except only partial irregularity in the fibrous sheath was observed. Furthermore, in the present work, GSE preserved the DNA integrity of the germ cells against damage induced by CP where strong PCNA-positive immunolabelled basal germ cell nuclei were recorded, indicating the progression of spermatogenesis. These results were also recorded by Morsi *et al*. (2020). This protective effect of GSE is based on its antioxidant activity due to its high resveratrol content, which protects the testicular parenchyma against ROS-induced lipid peroxidation in cell membranes and DNA damage (Truong *et al*., 2018). This explained the significant increase in GSH levels with a marked reduction in MDA levels in this study. These findings were supported by Mohamed and Aly (2014) and Abdel-kawi *et al*. (2016).

Conclusion

The histomorphometry, immunohistochemical and ultrastructural data confirmed that CP induced spermatogenesis arrest with oxidative DNA damage to germ cells. Interestingly, PSE and GSE markedly attenuate these harmful effects triggering improvements in the testicular antioxidant status, testicular histoarchitecture, and histomorphometric parameters of the seminiferous tubules as well as the proliferative state of germ cells, probably due to their powerful antioxidant activities.

Acknowledgments

The authors would like to thank all staff members of the Pathology Department, Faculty of Veterinary Medicine, Benha University.

Conflict of interest

The authors declare that they have no conflict of interest.

References

Abdel-Kawi, S.H., Hashem, K.S., Abd-Allah, S., 2016. Mechanism of diethylhexylphthalate (DEHP) induced testicular damage and of grape seed extract-induced protection in the rat. Food Chem. Toxicol. 90, 64-75. https://doi.org/10.1016/j.fct.2016.02.003

Aboul-Ela, E.I., Omara, E.A., 2014. Genotoxic and Histopathological Aspects of Treatment with Grape Seed Extract on Cancer Induced with Cyclophosphamide in Mice. Cell Biology. 2, 18-27. https://doi.org/10.11648/j.cb.20140203.11

Adana, M.Y., Imam, A., Bello, A.A., Sunmonu, O.E., Alege, E.P., Onigbolabi, O.G., Ajao, M.S., 2022. Oral thymoquinone modulates cyclophosphamide-induced testicular toxicity in adolescent Wistar rats. Andrologia. 54, e14368. https://doi.org/10.1111/and.14368

Adsul, S., Madkaikar, V., 2021. Pumpkin (*Cucurbita pepo*) seed. In B. Tanwar, A. Goyal, (eds.), Oilseeds: Health Attributes and Food Applications. Singapore, Springer, pp. 473–506.

Aghaei, S., Nikzad, H., Taghizadeh, M., Tameh, A.A., Taherian, A., Moravveji, A., 2014. Protective effect of Pumpkin seed extract on sperm characteristics, biochemical parameters and epididymal histology in adult male rats treated with Cyclophosphamide. Andrologia. 46, 927-935. https://doi.org/10.1111/and.12175

Badavi, M., Abedi, H.A., Dianat, M., Sarkaki, A.R., 2013. Exercise Training and Grape Seed Extract Co-Administration Improves Lipid Profile, Weight Loss, Bradycardia, and Hypotension of STZ-Induced Diabetic Rats. Int. Cardiovasc. Res. J. 7, 111-117.

Bancroft, J.D., Layton, C., 2019. 'The hematoxylin and eosin', In: S.K. Suvarna, C. Layton, & J. D. Bancroft, (eds.), Bancroft's Theory and Practice of Histological Techniques, 8th Ed. ElSevier, Philadelphia, pp. 126–138.

Cengiz, M., Sahinturk, V., Yildiz, S.C., Şahin, İ.K., Bilici, N., Yaman, S.O., Altuner, Y., Appak-Baskoy, S., Ayhanci, A., 2020. Cyclophosphamide induced oxidative stress, lipid per oxidation, apoptosis and histopathological changes in rats: Protective role of boron. J. Trace. Elem. Med. Biol. 62, 126574. https://doi.org/10.1016/j.jtemb.2020.126574

D'andrea, M., Lawrence, D., Nagele, R., Wang, C., Damiano, B., 2008. PCNA indexing as a preclinical immunohistochemical biomarker for testicular toxicity. Biotech. Histochem. 83, 211-220. https://doi.org/10.1080/10520290802521804

Dabbish, E., Scoditti, S., Shehata, M.N.I., Ritacco, I., Ibrahim, M.A.A., Shoeib, T., Sicilia, E., 2024. Insights on cyclophosphamide metabolism and anticancer mechanism of action: A computational study. J. Comput. Chem. 45, 663-670. https://doi.org/10.1002/jcc.27280

Elfiky, S., Elelaimy, I., Hassan, A., Ibrahim, H., Elsayad, R., 2012. Protective Effect of Pumpkin Seed Oil Against Genotoxicity Induced by Azathioprine. J. Basic. Applied. Zoology 65, 289-298. https://doi.org/10.1016/j.jobaz.2012.10.010

Ghafouri-Fard, S., Shoorei, H., Abak, A., Seify, M., Mohaqiq, M., Keshmir, F., Taheri, M., Ayatollahi, S.A., 2021. Effects of chemotherapeutic agents on male germ cells and possible ameliorating impact of antioxidants. Biomed. Pharmacother. 142, 112040. https://doi.org/10.1016/j.biopha.2021.112040

Ghobadi, E., Moloudizargari, M., Asghari, M.H., Abdollahi, M., 2017. The mechanisms of cyclophosphamide-induced testicular toxicity and the protective agents. Expert. Opin. Drug. Metab. Toxicol. 13, 525-536. https://doi.org/10.1080/17425255.2017.1277205

Gupta, M., Dey, S., Marbaniang, D., Pal, P., Ray, S., Mazumder, B., 2020. Grape seed extract: having a potential health benefits. J. Food. Sci. Technol. 57, 1205-1215. https://doi.org/10.1007/s13197-019-04113-w

Hamdi, H., 2020. Testicular Dysfunction Induced by Aluminum Oxide Nanoparticle Administration in Albino Rats and the Possible Protective Role of Pumpkin Seed Oil. J. Basic. Applied. Zoology. 81, 42. https://doi.org/10.1186/s41936-020-00178-8

Hashemi, J.M., 2013.Pumpkin Seed Oil and Vitamin E Improve Reproductive Function of Male Rats Inflicted by Testicular Injury. World. Applied. Sci. J. 23, 1351-1359. https://doi.org/10.5829/idosi.wasj.2013.23.10.13153

Hassanzadeh-Taheri, M., Hosseini, M., Dorranipour, D., Afshar, M., Moodi, H., Salimi, M., 2019. The Oleo-Gum-Resin of Commiphora Myrrha Ameliorates Male Reproductive Dysfunctions in Streptozotocin-Induced Hyperglycemic Rats. Pharm. Sci. 25, 294-302. https://doi.org/10.15171/PS.2019.49

Johnsen, S.G., 1970. Testicular biopsy score count--a method for registration of spermatogenesis in human testes: normal values and results in 335 hypogonadal males. Hormones 1, 2-25. https://doi.org/10.1159/000178170

Kamarzaman, S., Sha ban, M., Rahman, S.A., Rahman, S.A., 2013. Effects on Mouse Spermatogenesis and DNA Fragmentation Following Exposure to Cyclophosphamide and Thymoquinone. Eur. Int. J. Sci. Technol. 2, 119-136.

Karimi, S., Hosseinimehr, S.J., Mohammadi, H.R., Khalatbary, A.R., Amiri, F.T., 2018. Zataria multiflora ameliorates cisplatin-induced testicular damage via suppression of oxidative stress and apoptosis in a mice model. Iran. J. Basic. Med. Sci. 21, 607-614. https://doi.org/10.22038/IJBMS.2018.26784.6558

Lu, W.P., Mei, X.T., Wang, Y., Zheng, Y.P., Xue, Y.F., Xu, D.H., 2015. Zn(II)-curcumin protects against oxidative stress, deleterious changes in sperm parameters and histological alterations in a male mouse model of cyclophosphamide-induced reproductive damage. Environ. Toxicol. Pharmacol. 39, 515-24. https://doi.org/10.1016/j.etap.2014.12.014

Malek, M.A., Dasiman, R., Khan, N.A.M.N., Mohamed-Akhlak, S., Mahmud, M.H., 2022. The protective effects of Procyanidin C-1 on bisphenol a-induced testicular dysfunction in aged mice. Food. Sci. Human. Wellness. 11, 965-974. https://doi.org/10.1016/j.fshw.2022.03.020

Mohamed, N.Z., Aly, H.F., 2014. Chemotherapeutic Potential of Grape Seed Extract (*Vitis vinifera*) Against Cyclophosphamide-Induced Oxidative Stress in Mice. World. J. Pharm. Res. 3, 231-249.

Mohammadi, F., Nikzad, H., Taherian, A., Amini Mahabadi, J., Salehi, M., 2013. Effects of Herbal Medicine on Male Infertility. Anatomical Sci. J. 10, 3-16.

Morsi, A.A., Shawky, L.M., El Bana, E.A., 2020. The potential gonadoprotective effects of grape seed extract against the histopathological alterations elicited in an animal model of cadmium-induced testicular toxicity. Folia. Morphol. (Warsz). 79, 767-776. https://doi.org/10.5603/FM.a2020.0003

Mousa, H., Allam, A., Ali Mohamed, A., 2023. The Possible Protective Role of Crocin and Pumpkin Seed Oil against Lead-Induced Testicular Cytotoxicity in Adult Male Albino Rat.Hormonal, Histological and Immunohistochemical study. Benha Med. J. 40, 1-16. https://doi.org/10.21608/bmfj.2022.154319.1632

Moustafa, N., Abdul-Hamid, M., El-Nesr, K.A., Abukhadra, A.M., 2020.Protective Effect of Alpha Lipoic Acid and Royal Jelly Against the Side Effects of Cyclophosphamide in Testis of Male Albino Rats. Egyptian. J. Histol. 43, 539-553. https://doi.org/10.21608/EJH.2019.16643.1167

Myers, C.E., Hoelzinger, D.B., Truong, T.N., Chew, L.A., Myles, A., Chaudhuri, L., Egan, J.B., Liu, J., Gendler, S.J., Cohen, P.A., 2017. Chemotherapy can induce weight normalization of morbidly obese mice despite undiminished ingestion of high fat diet. Oncotarget. 8, 5426-5438. https://doi.org/10.18632/oncotarget.14576

Nimptsch, K., Platz, E.A., Willett, W.C., Giovannucci, E., 2012. Association between plasma 25-OH vitamin D and testosterone levels in men. Clin. Endocrinol. (Oxf). 77, 106-12. https://doi.org/10.1111/j.1365-2265.2012.04332.x

Ofoego, U., Nweke, E., Chioma, O., 2019. Co-Administration of Cyclophosphamide and Ethanolic Seed Extract of Telfairia Occidentalis (Pumpkin) Protects Testicular Functions in Adult Male Albino Wistar Rats. World J. Pharm. Res. 8, 325-342. https://doi.org/10.20959/wjpr20193-14356

Oliveira, R.J., Cunha-Laura, A.L., Gonçalves, C.A., Monreal, A.C.D., Costa, D.S., Meza, A., De Lima, D.P., Beatriz, A., Amaral, E.A., Auharek, S.A., 2020. Effects of 3-Heptyl-3,4,6-trimethoxy-3H-isobenzofuran-1-one alone or/in association with cyclophosphamide on testicular function. Andrologia. 52, e13622. https://doi.org/10.1111/and.13622

Pan, J., Zhang, J., 2021. Research Progress of PCNA in Reproductive System Diseases. Evid. Based Complement. Alternat. Med. 2391917. https://doi.org/10.1155/2021/2391917

Potnuri, A.G., Allakonda, L., Lahkar, M., 2018. Crocin attenuates cyclophosphamide induced testicular toxicity by preserving glutathione redox system. Biomed. Pharmacother. 101, 174-180. https://doi.org/10.1016/j.biopha.2018.02.068

Salimnejad, R., Rad, J.S., Nejad, D.M., 2018. Protective Effect of Ghrelin on Oxidative Stress and Tissue Damages of Mice Testes Followed by Chemotherapy with Cyclophosphamide. Crescent. J. Medical. Biol. Sci. 5, 138-43.

Shaban, A., Sahu, R.P., 2017. Pumpkin Seed Oil: An Alternative Medicine. Int. J. Pharmacogn. Phytochem. Res. 9, 11. https://doi.org/10.25258/phyto.v9i2.8066

Singh, M., Kumar, N., Shuaib, M., Garg, V. K., Sharma, A., 2014. A review on renal protective agents for cyclophosphamide induced nephrotoxicity. World J. Pharm. Pharmaceut. Sci, 3, 737-747.

Sönmez, M.F., Tascioglu, S., 2015. Protective effects of grape seed extract on cadmium-induced testicular damage, apoptosis, and endothelial nitric oxide synthases expression in rats. Toxicol. Ind. Health. 32, 1486-1494. https://doi.org/10.1177/0748233714566874

Srivastava, N., Sahu, P., Banerjee, M., 2021. Nutraceutical Potential of Pumpkin (Cucurbita sp.) Powder, Seed, Extracts, and Oil on Diabetes: Mini Review. J. Endo and Dis. 5(1). https://doi.org/10.31579/2640-1045/063

Tabeshpour, J., Mehri, S., Shaebani Behbahani, F., Hosseinzadeh, H., 2018. Protective effects of *Vitis vinifera* (grapes) and one of its biologically active constituents, resveratrol, against natural and chemical toxicities: A comprehensive review. Phytother. Res. 32, 2164-2190. https://doi.org/10.1002/ptr.6168

Taghizadeh, F., Hosseinimehr, S.J., Zargari, M., Karimpour Malekshah, A., Talebpour Amiri, F.B., 2020. Gliclazide attenuates cisplatin-induced nephrotoxicity through inhibiting NF-κB and caspase-3 activity. IUBMB Life. 72, 2024-2033. https://doi.org/10.1002/iub.2342

Teilmann, A.C., Nygaard Madsen, A., Holst, B., Hau, J., Rozell, B., Abelson, K.S.P., 2014. Physiological and pathological impact of blood sampling by retro-bulbar sinus puncture and facial vein phlebotomy in laboratory mice. PLoS One. 9, e113225. https://doi.org/10.1371/journal.pone.0113225

Tohamy, H.G., El-Kazaz, S.E., Alotaibi, S.S., Ibrahiem, H.S., Shukry, M., Dawood, M.A.O., 2021. Ameliorative Effects of Boswellic Acid on Fipronil-Induced Toxicity: Antioxidant State, Apoptotic Markers, and Testicular Steroidogenic Expression in Male Rats. Animals (Basel). 11, 1302. https://doi.org/10.3390/ani11051302

Torabi, F., Malekzadeh Shafaroudi, M., Rezaei, N., 2017. Combined protective effect of zinc oxide nanoparticles and melatonin on cyclophosphamide-induced toxicity in testicular histology and sperm parameters in adult Wistar rats. Int. J. Reprod. Biomed. 15, 403-412.

Truong, V.L., Jun, M., Jeong, W.S., 2018. Role of resveratrol in regulation of cellular defense systems against oxidative stress. Biofactors. 44, 36-49. https://doi.org/10.1002/biof.1399

Vinayashree, S., Vasu, P., 2021. Biochemical, nutritional and functional properties of protein isolate and fractions from pumpkin (Cucurbita moschata var. Kashi Harit) seeds. Food Chem. 340, 128177. https://doi.org/10.1016/j.foodchem.2020.128177

Woods, A.E., Stirling, J.W., 2019. 'Transmission electron microscopy', In: S. K. Suvarna, C. Layton, & J. D. Bancroft, (eds.), Bancroft's Theory and Practice of Histological Techniques, 8th Ed. ElSevier, Philadelphia, pp. 434–475.

Xanthopoulou, M.N., Nomikos, T., Fragopoulou, E., Antonopoulou, S., 2009. Antioxidant and lipoxygenase inhibitory activities of pumpkin seed extracts. Food Res. Inter. 42, 641-646. https://doi.org/10.1016/j.foodres.2009.02.003

Zhao, H., Jin, B., Zhang, X., Cui, Y., Sun, D., Gao, C., Gu, Y., Cai, B., 2015. Yangjing Capsule Ameliorates Spermatogenesis in Male Mice Exposed to Cyclophosphamide. Evid. Based. Complement. Alternat. Med. 2015, 980583. https://doi.org/10.1155/2015/980583

Zirak, M.R., Mehri, S., Karimani, A., Zeinali, M., Hayes, A.W., Karimi, G., 2019. Mechanisms behind the atherothrombotic effects of acrolein, a review. Food Chem. Toxicol. 129, 38-53. https://doi.org/10.1016/j.fct.2019.04.034